University Library



A gateway to Melbourne's research publications

Minerva Access is the Institutional Repository of The University of Melbourne

Author/s:
Wasko, C;Shao, Y;Vogel, E;Wilson, L;Wang, QJ;Frost, A;Donnelly, C

Title:
Understanding trends in hydrologic extremes across Australia

Date:
2021-02-01

Citation:
Wasko, C., Shao, Y., Vogel, E., Wilson, L., Wang, Q. J., Frost, A. & Donnelly, C. (2021). Understanding trends in hydrologic extremes across Australia. Journal of Hydrology, 593, https://doi.org/10.1016/j.jhydrol.2020.125877.

Persistent Link:
https://hdl.handle.net/11343/264214

Understanding trends in hydrologic extremes across Australia

Conrad Wasko[1*], Yawen Shao[1], Elisabeth Vogel[2], Louise Wilson[2], QJ Wang[1], Andrew Frost[3], Chantal Donnelly[4]

[1]Department of Infrastructure Engineering, The University of Melbourne, Parkville, Australia

[2]Australian Bureau of Meteorology, Melbourne, Australia

[3]Australian Bureau of Meteorology, Sydney, Australia

[4]Australian Bureau of Meteorology, Brisbane, Australia

*conrad.wasko@unimelb.edu.au

Key points:

Australian Landscape Water Balance model is used to evaluate hydrologic trends

Trends in modelled streamflow are evaluated against observed streamflow

Rainfall, soil moisture, and streamflow trends are consistent with tropical expansion

Changes in flood and drought are linked to mean rainfall changes at continental scale

Trends are more likely to be driven by local factors at the catchment scale

Key words:

Australia, rainfall, runoff, soil moisture, drought, flood, climate change, trend, AWRA-L

Abstract

Changes in the hydrologic cycle have far reaching impacts on agricultural productivity, water resources availability, riverine ecosystems, and our ability to manage environmental assets, bushfire risk, and flood hazard. For example, declining rainfall in the southeast of Australia has led to a prolonged period of drought, with serious impacts on agriculture, the environment, and water supply to urban and rural towns. Here, using the continental wide Australian Water Resources Assessment Landscape model (AWRA-L), we evaluate historical trends from 1960 to 2017 in rainfall, soil moisture, evapotranspiration, and runoff to explain changing drought and flooding. Northern parts of Australia have experienced increasing annual rainfall totals, resulting in increased water availability in the tropics with increased soil moisture, evapotranspiration, and runoff, particularly during the hot, wet monsoon season. In contrast, the southwest and southeast coast of Australia have experienced declines in rainfall, particularly in the colder months, corresponding with decreasing evapotranspiration, soil moisture, and runoff. Trends in flooding are aligned with runoff trends, and closely follow trends in rainfall, with changes in soil moisture of secondary influence. Streamflow droughts, measured by the standardised runoff index, are increasing across large parts of Australia, with these increases more widespread than changes in rainfall alone. Increases in rainfall in the tropics of northern Australia appear to be related to decreasing drought occurrence and extent, but this trend is not universal, suggesting changes in rainfall alone are not an indicator of changing drought conditions.

1 Introduction

1.1 Changes in the global hydrological cycle

One of the most important questions in hydrology is how the hydrologic cycle is being impacted by climate change (Huntington, 2006; Koutsoyiannis, 2020). Water in the landscape and rivers is essential for: agriculture, town and industrial water supply, the environment, cultural values, recreation, hydropower and more; hence changes to when and where water is available has far reaching impacts. In terms of hydrologic extremes, flood and droughts are among the costliest natural disasters in the world, causing risk to life, food security and, in the case of drought, increased bushfire risk.

Globally, precipitation has increased as per energy constraints (Allan et al., 2020; Allen and Ingram, 2002) at approximately 2.4mm/decade (Becker et al., 2013; Hartmann et al., 2013) in line with climate model projections of a 2% increase in precipitation per degree increase in global mean temperature (Kharin et al., 2013). Most of the increases in precipitation have occurred over tropical areas with decreases elsewhere (Beck et al., 2019), while precipitation extremes such as annual maxima of daily rainfall have increased universally at a rate close to 7% per degree increase in global mean temperature (Sun et al., 2020; Westra et al., 2013). There is evidence that, consistent with changes in rainfall, soil moisture has experienced wetting trends in the tropics and drying trends in the extra tropics (Feng and Zhang, 2015; Liu et al., 2019) but trends differ depending on the data set used (Albergel et al., 2013).

Compared to changes in annual average conditions, changes in hydrological extremes are more challenging to quantify and understand. Increasing temperatures have increased the likelihood of drought conditions in many regions of the world (Hartmann et al., 2013; Liu et al., 2019), though again, results differ depending on the index used (Asadi Zarch et al., 2015). Despite many studies pointing to increases in extreme precipitation (Donat et al., 2013; Groisman et al., 2005; Martinez-Villalobos and Neelin, 2018; Sun et al., 2020; Westra et al., 2013), there is a very mixed trend in flood response (Sharma et al., 2018) with more sites globally showing decreases in flooding than increases (Do et al., 2017). Despite this variability, trends in high flows follow average annual flow trends both globally (Gudmundsson et al., 2019) and across Australia (Zhang et al., 2016). In regions free of snow-melt, it has been postulated that changes in flooding are due to changing antecedent soil moisture conditions (Ivancic and Shaw, 2015; Sharma et al., 2018; Wasko et al., 2019). However, few studies have studied trends in antecedent conditions explicitly (Tramblay et al., 2019; Wasko and Nathan, 2019a).

1.2 Hydrological trends in Australia

Australia forms a valuable test case for investigating the impacts of climate change on the hydrologic cycle. It straddles the tropics and extratropics, experiencing a wide range of climates, and is largely free of snowmelt. In addition, trends in Australian precipitation and temperature reflect global patterns (Alexander et al., 2007), although streamflow exhibits extremely high variability compared to the rest of the world (Chiew and McMahon, 2002; McMahon et al., 2007; Peel et al., 2004).

Mean annual rainfall has increased in the tropical north of Australia and decreased in the south (Dey et al., 2019), particularly along the south-east and south-west coasts due to changed cutoffs and frontal systems (Risbey et al., 2013) consistent with a tropical expansion (Grise et al., 2018; Staten et al., 2018). For example, south-western Australia has undergone decreased cool season rainfall in April to October, with sharp decreases in May-July rainfall since 1970. There has been a similar decline of rainfall over south-eastern Australia in April to October rainfall since the late 1990s. Meanwhile, in northern Australia, there has been an observed rainfall increase since the 1970s, especially in the northwest (CSIRO & BOM, 2018).

Since the 1950s increasing streamflow in the northern tropics and decreasing streamflow over southern Australia has been observed (Zhang et al., 2016). Across Australia studies of trends in evapotranspiration show mixed trends temporally and spatially. Prior to 1999, decreasing trends in observed pan evaporation across Australia were linked to declining wind speeds (Johnson and Sharma, 2010), but since then, many sites have shown increased pan evaporation, possibly due to an increased vapor pressure deficit (Stephens et al., 2018). Despite increases in global estimates of terrestrial evapotranspiration (Zeng et al., 2018), evapotranspiration estimates derived from remote sensing and flux towers show a decrease in evapotranspiration between 1998-2008 attributed to moisture limitations (Jung et al., 2010).

There is a large discrepancy in trends calculated between different soil moisture products, but in general datasets point to more severe droughts in arid and semi-arid regions (Liu et al., 2019). Using data obtained from the European Space Agency, soil moisture was found to be decreasing across Australia between 1979 and 2013, with the exception of the tropical north (Feng and Zhang, 2015). However, another study for 1988–2010 using multiple reanalysis and satellite derived data sets indicated largely conflicting results between data sets, particularly at the regional scale (Albergel et al., 2013). This may be because reanalysis data sets, particularly ERA-INTERIM, have large rainfall biases (Andersson et al., 2015; Weedon et al., 2014) while remote sensed data sets measure soil moisture at different depths (Holgate et al., 2016).

The magnitude of extreme hourly and daily rainfall, across a range of exceedance thresholds, has increased over the last half a century across Australia (Alexander and Arblaster, 2017; Guerreiro et al., 2018) with shifts to a greater frequency of longer duration events in the tropics and shorter duration events in extra-tropics (Dey et al., 2020). Despite more evidence for increasing rainfall extremes compared to decreases, more streamflow gauging sites show decreases in annual maxima than increases (Ishak et al., 2013; Zhang et al., 2016). Decreased flooding has been attributed to decreased antecedent soil moisture prior to the onset of the storm events across southern parts of Australia (Wasko and Nathan, 2019a). This demonstrates how a better understanding of the drivers of changes on streamflow and flooding, that is, rainfall, evapotranspiration and soil moisture, and how they interact, is required to better predict the likely impacts of climate change on the hydrological cycle, and subsequently economic activity, the environment, communities, and ecosystems (Berghuijs et al., 2019).

1.3 Research gap in understanding drivers of concurrent hydrological trends

Due to the greater number of rainfall gauging stations and observations compared to streamflow, studies often infer impacts to flooding from changes in rainfall. However, this approach may lead to apparent contradictions such as increasing rainfall extremes which are not associated with increased flooding (Sharma et al., 2018). Few studies examine hydroclimatic variables in unison (exceptions include, Johnson et al., 2016; Wasko et al., 2020; Wasko and Nathan, 2019a) and of those that do, most focus on instrumented catchments and the Millennium Drought (2001-2009) in the south-east of Australia (Fowler et al., 2016; King et al., 2020; Kirono et al., 2017; Potter et al., 2010; Saft et al., 2016, 2015; Van Dijk et al., 2013). As such, a holistic understanding of concurrent changes in hydroclimatic variables across Australia does not currently exist. Here, we use a high-resolution continental water balance model to study trends in simulated streamflow across the Australian continent, along with drought and high flow (flood) indices, according to their key drivers: rainfall, evapotranspiration, and soil moisture. We test the model's ability to reproduce hydrological trends then use the model as a tool to quantify historical trends across the water balance.

2 Methodology

The approach used for this study is as follows:

1. The Australian Water Resource Assessment -Landscape model (AWRA-L) model is assessed in terms of simulated runoff reproduction of streamflow trends at a set of high-quality catchments; with catchment trend assessment grouped according to climatologically similar regions;

2. Spatial trends in simulated runoff (aggregated to streamflow) are compared to trends in rainfall, potential evaporation (PET), actual evapotranspiration (AET), and soil moisture.
3. Trends in catchment scale runoff extremes (drought and flood indices) are compared to trends in related hydrologic and climate indices (i.e. mean rainfall and soil moisture trends, and trends in extreme rainfall).

2.1 AWRA-L Model

AWRA-L is a daily, gridded, one-dimensional, semi-distributed continental-scale landscape water balance model developed by the CSIRO and the Australian Bureau of Meteorology (BOM) (Frost et al., 2018; Van Dijk, 2010; Viney et al., 2015) for water resource assessment and monitoring. It is currently run operationally to provide near real-time hydrological data at a resolution of 0.05° x 0.05° (approximately 5km x 5km) from 1911 to the present across Australia (see www.bom.gov.au/water/landscape). Figure 1 presents the climate inputs, hydrological outputs, and simulated processes in AWRA-L.

The model forcing inputs are daily solar radiation, minimum and maximum temperature, 2m wind speed, and precipitation. Other static inputs describe the spatial variability of soil and geological properties and land use. In its operational use, AWRA-L uses daily precipitation and maximum and minimum temperatures obtained from the Australian Water Availability Product (AWAP) (Jones et al., 2009), remotely-sensed solar radiation (Grant et al., 2008), and an interpolated field of station-based observations of wind speed (McVicar et al., 2008). Daily varying climatologies of solar radiation and wind speed are used prior to 1990 and 1975, respectively, prior to the relevant observational datasets becoming available.

The key hydrologic processes modelled include: 1) portioning of rainfall between interception and water contributing to the water balance; 2) infiltration or saturation excess surface runoff dependent on groundwater saturation; 3) interflow, drainage, and evaporation from the soil layers; and 4) baseflow and evapotranspiration from the groundwater store. Potential evaporation is modelled using the Penman equation (Penman, 1948), which uses wind and temperature as inputs, along with solar radiation to calculate the terrestrial energy balance following Donohue el al. (2010). The soil is modelled in three layers (0-0.1m, 0.1-1m, and 1-6m depth) with differing model parameters between layers. Shallow rooted vegetation has access to soil moisture in the upper two layers while deep rooted vegetation also has access to the bottom most layer. Key output fluxes are runoff, actual evapotranspiration, and soil moisture for the three soil layers and deep drainage to the groundwater store. Similar to other semi-distributed

models, the total runoff from a grid cell is a summation of the surface and subsurface runoff fluxes. AWRA-L contains 49 parameters, of which 28 are fixed according to previous parameter sensitivity experiments and prior knowledge, and 21 are optimised to maximise an objective function that considers performance against observed streamflow (covering the period 1981-2011), remotely sensed evapotranspiration, and remotely sensed surface soil moisture at a set of 295 unimpaired catchments (Zhang et al., 2011). The reader is referred to Viney et al. (2015) and Frost et al. (2018) for further details.

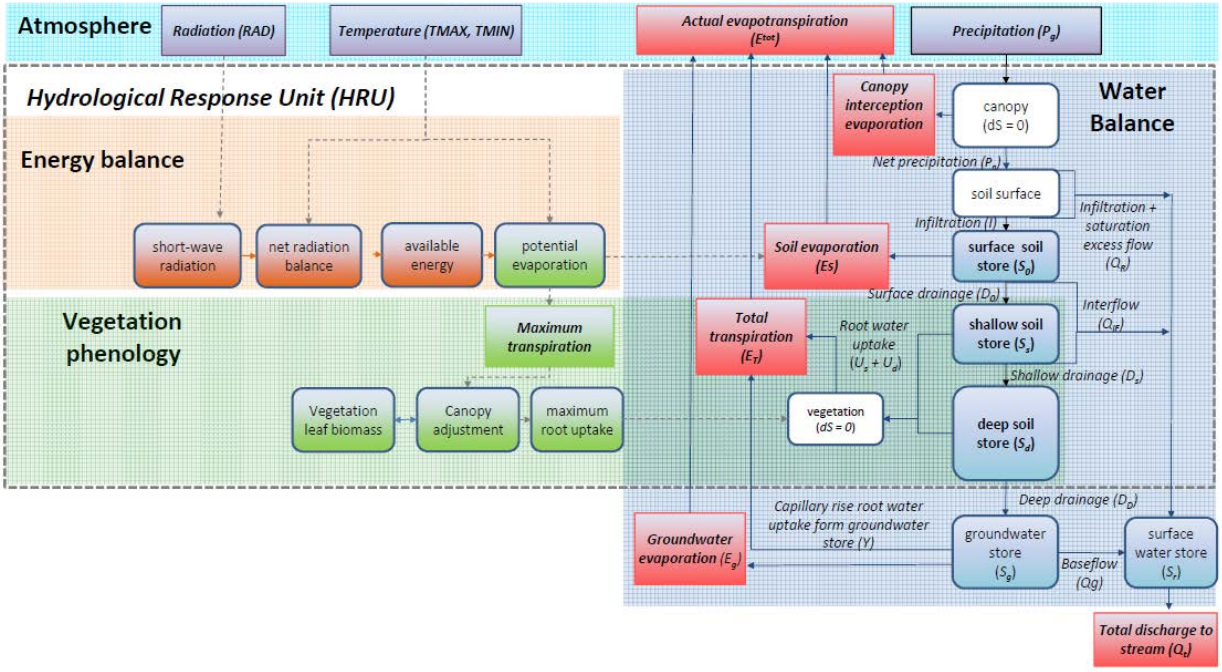


Figure 1. AWRA-L conceptual structure. Purple: climate inputs; Blue rounded boxes: water stores; Red boxes: water flux outputs; Brown: energy balance; Green rounded boxes: vegetation processes. The dotted line indicates processes modelled in each grid cell (Frost et al., 2018).

Verification is undertaken firstly to the calibration data at independent sites (streamflow and remotely sensed estimates of catchment average soil moisture and evapotranspiration over a separate set of 291 unimpaired catchments); along with in-situ measurements of soil moisture, flux tower estimates of evapotranspiration, and estimates of groundwater recharge nationally; see Frost and Wright (2018). AWRA-L performs well compared to other available continental scale models for streamflow (predominantly due to streamflow data being used in calibration), and similarly to locally calibrated nearest-neighbour regionalised conceptual rainfall runoff models, giving confidence that AWRA-L can be

considered a fit-for-purpose continental scale hydrological model for water resource and agricultural applications. Similarly, AWRA-L compares well to continental scale models when assessed against in-situ root-zone (0-90cm) soil moisture observations, and shows comparable (if not better) correlation to in-situ and remotely sensed data (Holgate et al., 2016), with soil moisture variability representative of catchment dynamics (Peterson et al., 2020). AWRA-L shows comparable performance over other continental scale models for evapotranspiration but currently shows slightly poorer performance according to annual correlation of deep drainage (Frost and Wright, 2018).

As a result of this performance across the water balance, AWRA-L forms an integral part of the Australian Bureau of Meteorology's national water accounting, water monitoring (Elmahdi et al., 2016; Hafeez et al., 2015), and estimation of antecedent conditions for event-based flood forecasting. It has been used in retrospective studies for national flood design guidelines (Ball et al., 2019), to understand the impact of changes in soil moisture on flood magnitude (Wasko and Nathan, 2019a) and flood timing (Wasko et al., 2020), and for the identification of flash drought using the evaporative stress index (Nguyen et al., 2019).

2.2 Analysis

2.2.1 Regional grouping

Broadly, Australia's climate varies from tropical in the north to temperate in the south with an arid climate inland. The north generally receives monsoon-driven rainfall in warmer months (November to April) with little to no rainfall in the colder months (May to October), with rainfall becoming more seasonally uniform moving south. The exception is the south-east which experiences a dry austral summer and wet colder months. A small mountain range that runs along the east coast of Australia demarcates regions with less rainfall inland and more rainfall towards the coast. Recognising these differences in climate, we (regionally) aggregate and discuss results based on clusters of Natural Resource Management (NRM) regions. For consistency with the other work in Australia (CSIRO and Bureau of Meteorology, 2015) the NRM regions are defined by catchments and bioregions of similar climatic conditions (Figure 2). We note that the Murray Basin region presented here forms the lower part of the larger Murray Darling Basin, one of the most significant agricultural regions in Australia.

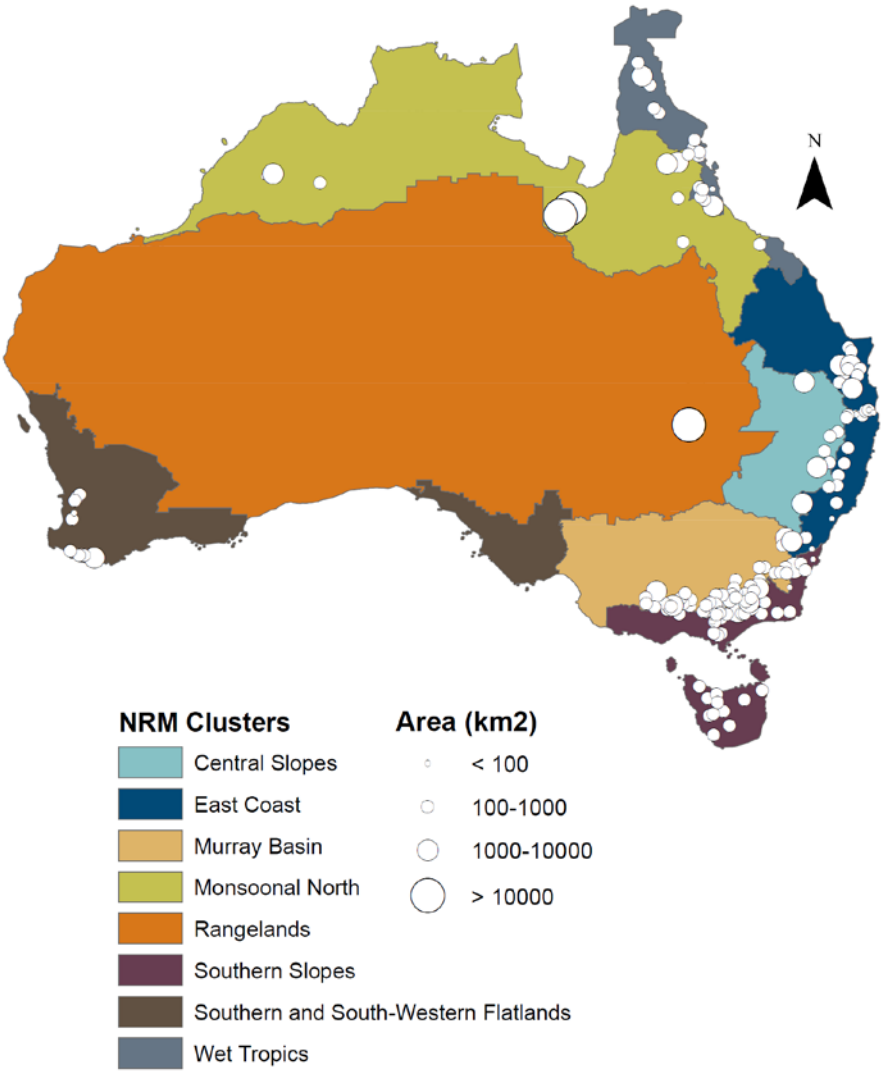


Figure 2. Hydrologic reference stations underlain by Natural Resource Management (NRM) regions.

2.2.2 Evaluation of simulated streamflow trends

Although AWRA-L has been extensively validated, the ability of AWRA-L to capture observed hydrological trends has not been previously tested. Observed (historical) trends in potential evapotranspiration (PET), actual evapotranspiration (AET), and soil moisture (SM) are traditionally inconsistent and data source dependent (see Section 1.2). For this reason, and because streamflow is an integration of the above fluxes and stores, we focus on evaluating trends in catchment-aggregated AWRA-L runoff representing streamflow. It is reasonable to assume that the unrouted, simulated runoff can be aggregated to

represent streamflow in smaller catchments where streambed losses are smaller and routing impacts less. Simulated trends in catchment-aggregated AWRA-L runoff are evaluated against trends in observed monthly streamflow at a set of high quality observational hydrologic reference stations (Zhang et al., 2016). These stations represent relatively unaltered catchments (low urbanisation, irrigation, forestry effects). In total 160 stations of varying length are used. Most stations have recordings beginning in the 1970s with the longest length of record 37 years, shortest 19 years, and a median record length of 35 years. Station locations are presented in Figure 2 with the reader referred to Zhang et al. (2016) for further details of this data set.

2.2.3 Trends in simulated hydroclimatic variables and indicators of flood and drought

Trends in observed streamflow, rainfall (AWAP), and simulated PET, AET, soil moisture, and runoff are calculated as the slope of a linear regression of the seasonal or annual means of the respective variable. Results focus on the period 1960-2017, coinciding with the increase in temperature identified post 1960 due to anthropogenic climate change (Fawcett et al., 2012). Here, we analyse root-zone soil moisture (0-100cm soil depth), as it is most correlated with catchment flood response (Hill et al., 2016; Hill and Thomson, 2019) modulating streamflow at various levels of event severity (Wasko et al., 2020; Wasko and Nathan, 2019a).

Trends in high (flood) and low (drought) flow indicators were also examined and compared to trends in rainfall and evapotranspiration and runoff. Here we use the 90th percentile (q90) of annual daily flow and 5-day (5day) annual maxima for high flows/floods. The standardised runoff index (SRI) is used to characterise drought (Shukla and Wood, 2008). The SRI is defined by fitting a probability distribution to the runoff time-series (in this case either gamma, log-normal, or normal based on the best fit) and converting the fitted cumulative distribution to a standard normal deviate. Here, the SRI-12 (based on a 12-month calendar year aggregate) is used. The definitions, or classifications, of drought (McKee et al., 1993) according to SRI-12 are presented in Table 1. As an indicator of drought extent, for each NRM region the trend in the proportion of grid cells experiencing drought, as defined by the SRI-12 categories presented in Table 1, is also calculated.

Table 1. Classification of drought category using the standardised runoff index (SRI)

SRI Value	Drought Category	Time in category (%)
-1.00 to -1.49	Moderate	9.2
-1.50 to -1.99	Severe	4.4

-2 or less	Extreme	2.3

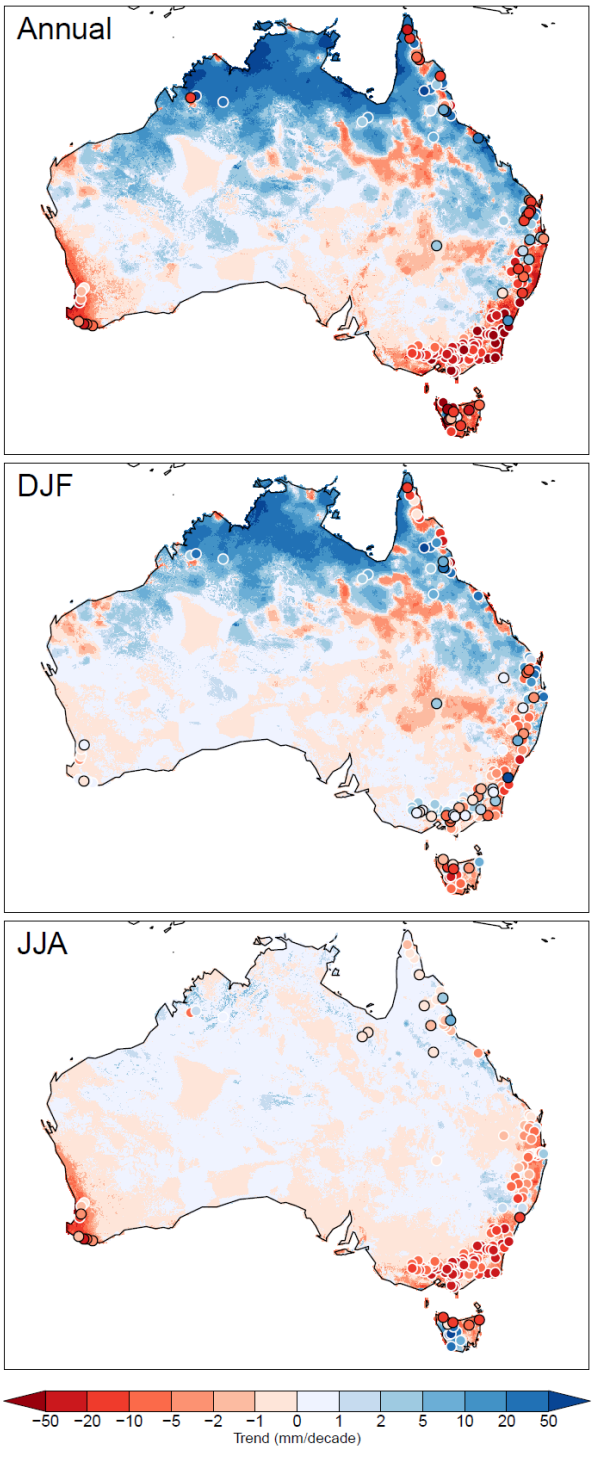
3. Results

The results are presented as follows: first AWRA-L streamflow trends are evaluated against observed trends. Next the continental scale trends in seasonal and annual means of AWAP (observed) rainfall, and simulated PET, AET, soil moisture, and runoff are presented. Trends in indicators of flood/drought are also evaluated. Finally, results are regionally aggregated across NRM regions. Trends are presented as scatter plots between variables to understand how trends interact at catchment scale, whether there are differences in the interaction regionally, and how these interactions compare to interactions at the continental scale.

3.1 Catchment streamflow trend verification

The observed streamflow trend underlain by simulated AWRA-L runoff for 1960 to 2017 is presented in Figure 3. Circles with white outline indicate that the direction of observed and modelled trends matches, whereas black circles indicate the direction of trends does not match. Although AWRA-L runoff on a grid cell basis is not directly comparable to streamflow which is a catchment outflow, regional coherence of observed and modelled trends is promising. On an annual basis AWRA-L runoff and observed streamflow in the south-west and south-east of the continent show strong decreasing trends. In the central north of the continent there are increasing trends both in observations and simulations, but simulations of the north-east coast display some divergence from observations. There appears to be localised decreases in observed streamflow along the north-east coast and at the very far south-west tip of the continent which are not captured by AWRA-L.

In the north of the continent, rainfall and streamflow is warm month dominant (DJF). The local variations in streamflow appear to be better captured in the north-east of the country which is promising as these are the months of largest trend. In the south of the country, where the trends are now small, there is localised increasing runoff modelled matching the observed trends for some locations. In the south of the continent, rainfall and streamflow is winter (JJA) dominant, and the strong decreasing trends are simulated well. For Tasmania, the island off the south-east coast of Australia, the strong gradient in observed trends between the east and west coast is captured (although being slightly displaced). For the northern winter (JJA) there is little trend and the modelled runoff likewise shows little trend. The general small but decreasing trend for winter runoff along the east coast moving north is captured.



264

265 **Figure 3.** Observed trends in streamflow for 160 HRS catchments across Australia underlain by
266 simulated AWRA-L runoff. Results are presented annually, for the austral summer months (DJF), and the
267 austral winter (JJA). White circles indicate that the direction of the modelled trend and observed trend

match. Black circles indicate that the direction of the modelled trend and observed trend does not match. For consistency, the runoff trend is for 1960 to 2017.

Seasonal and annual linear trends in simulated AWRA-L aggregated runoff (streamflow) are compared with observed streamflow on a catchment by catchment basis in Figure 4. For each catchment the modelled streamflow is a summation of the runoff for all the grid cells within the catchment (Section 2.2.2). Performance is compared on the basis of the NRM regions presented in Figure 2, noting that we assume the catchments are representative of the climatic conditions in that region. The coefficient of determination (r^2) and the hit rates annually and for each season are presented in Table 2. The hit rate corresponds to when the direction is correctly modelled, that is, the observed and simulated trends are both in the top-right (positive-positive) or bottom-left (negative-negative) quadrants in Figure 4. Simulated annual flow direction trend matches that observed at 122 of the 160 (76%) sites with an overall coefficient of determination of 0.38 (Table 2). In particular, the direction of simulated trend matches the observed for all sites in the Murray Basin, and good correspondence is found for the Southern Slopes with 76% of the sites matching in simulated and modeled trend direction. For the Monsoonal North, despite 82% sites matching in trend direction, the coefficient of determination is low due to a large scatter in the observed and modelled trends (Figure 4).

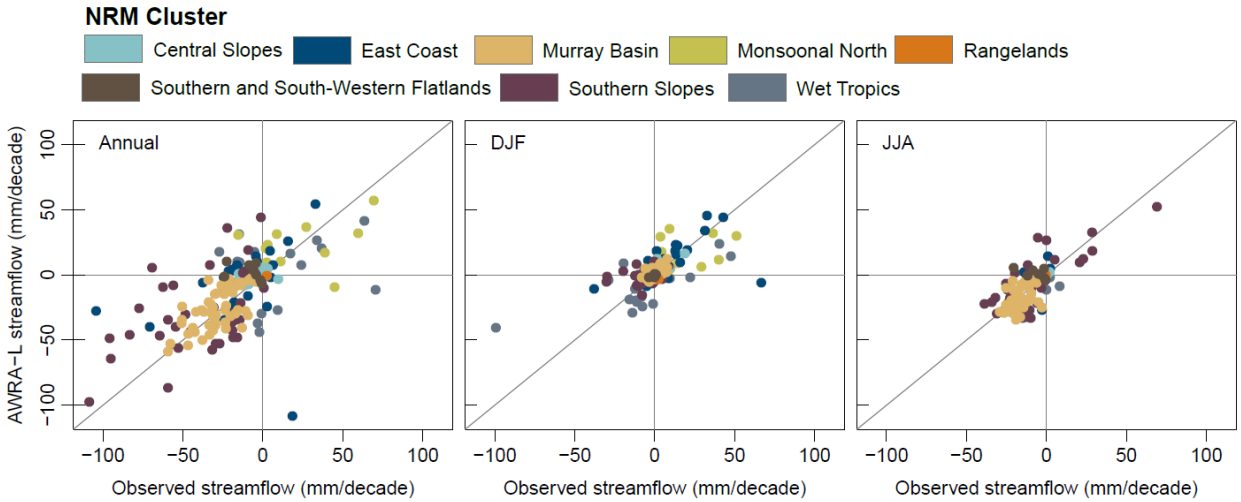


Figure 4. Scatter plot of simulated and observed trends in seasonal and annual runoff for 160 HRS catchments across Australia. Catchment locations are shown in Figure 3. Results are presented annually, for the austral summer months (DJF), and the austral winter (JJA). The hit rate and coefficient determination for each of the regions is presented in Table 1.

289 **Table 2.** The number of sites where the modelled catchment streamflow trends matches the observed
290 catchment streamflow trend (hit rate) and the coefficient of determination (r^2) between the modelled
291 and observed trends. Results are presented annually, for the austral summer months (DJF), and the
292 austral winter (JJA).

NRM Region	Hit rate (%)	r^2
Annual		
Wet Tropics	10 out of 17 (59%)	0.05
Monsoonal North	9 out of 11 (82%)	0.07
East Coast	14 out of 26 (54%)	0.08
Central Slopes	6 out 10 (60%)	0.30
Southern Slopes	25 out of 33 (76%)	0.26
Murray Basin	53 out of 53 (100%)	0.44
Rangelands	0 out of 1 (0%)	-
Southern and South-Western Flatlands	5 out of 9 (56%)	0.21
Overall	122 out of 160 (76%)	0.38
DJF		
Wet Tropics	14 out of 17 (82%)	0.54
Monsoonal North	11 out of 11 (100%)	0.06
East Coast	20 out of 26 (77%)	0.33
Central Slopes	8 out 10 (80%)	0.67
Southern Slopes	21 out of 33 (64%)	0.03
Murray Basin	41 out of 53 (77%)	0.34
Rangelands	0 out of 1 (0%)	-
Southern and South-Western Flatlands	7 out of 9 (78%)	0.37
Overall	122 out of 160 (76%)	0.43
JJA		
Wet Tropics	14 out of 17 (82%)	0.24
Monsoonal North	6 out of 11 (55%)	0.43
East Coast	25 out of 26 (96%)	0.13
Central Slopes	10 out 10 (100%)	0.25
Southern Slopes	28 out of 33 (85%)	0.59

Murray Basin	53 out of 53 (100%)	0.38
Rangelands	1 out of 1 (100%)	-
Southern and South-Western Flatlands	4 out of 9 (44%)	0.34
Overall	141 out 160 (88%)	0.55

293

294 The overall annual results can mask the results for the dominant streamflow season (Table 1). For summer
295 (DJF), the r^2 between trends is 0.06 and 0.54 for the Monsoonal North and Wet Tropics respectively,
296 however 11 of 11 sites (100%) in the Monsoonal North, and 14 out of 17 sites (82%) in the Wet Tropics
297 model the observed trend direction suggesting better correspondence in the summer (wet) months than
298 when streamflow is aggregated for the year. Good correspondence is observed for the East Coast and
299 Central Slopes in the winter (JJA) where AWRA-L simulates the observed trend direction at 35 of 36 sites.
300 Similarly, for the Murray Basin, all sites have the same modelled trend direction in the winter (the
301 dominant streamflow season). In comparison, in the summer, where there is the least flow, 41 out of 53
302 Murray Basin sites correctly model the observed trend direction (77%). Streamflow is winter dominant in
303 the Southern Slopes. Here 28 out of 33 (85%) sites model the correct trend direction with an r^2 of 0.59. At
304 the catchment scale, the Southern and South-Western Flatlands exhibit the lowest skill, with the correct
305 direction modelled at only 4 out of the 9 sites in the winter, possibly due to very differing local geology.

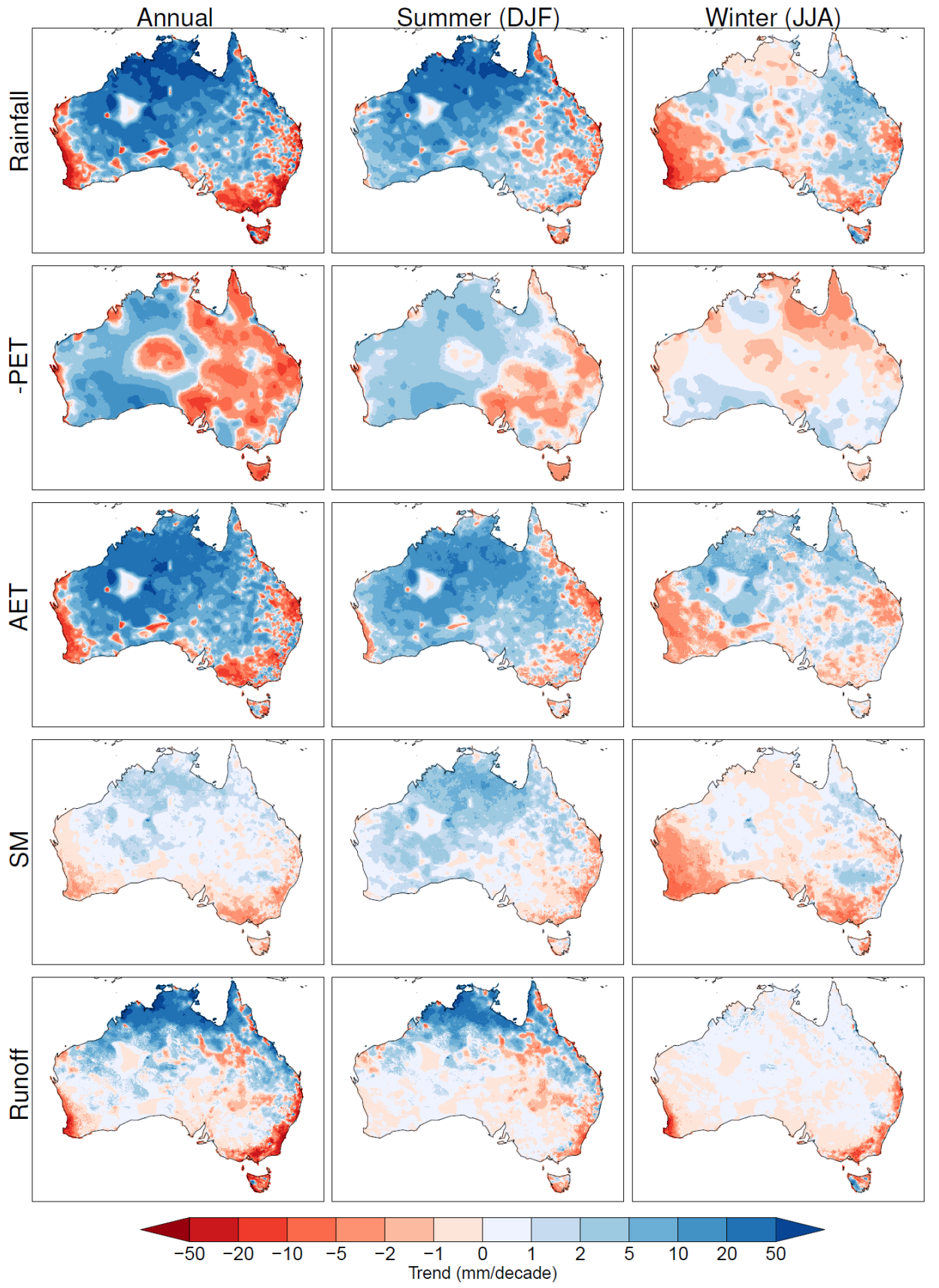
306 Overall, the modelled and observed trends compare well (Figure 3). At a majority of observational sites,
307 streamflow trends are reproduced by AWRA-L, giving confidence in using simulated water balance
308 variables to support our interpretations of the observed trends. The direction of the streamflow trend is
309 well reproduced, particularly for the dominant streamflow season, but the magnitude of the trend is not
310 necessarily represented well in parts of the tropics. Best correspondence is found in the south-east of the
311 country (Murray Basin and Southern Slopes regions). Evaluation was also performed for the 90th percentile
312 of streamflow with results largely similar to those presented here.

313 **3.2 Continental scale trends in hydroclimatological variables**

314 Having established the verification of AWRA-L, trends in the (simulated) hydrologic variables are now
315 evaluated. Figure 5 presents the trend in observed rainfall (derived from the gridded interpolated climate
316 observations) as well as simulated potential and actual evapotranspiration, soil moisture, and runoff for
317 the period 1960 to 2017. Two key points are noticeable for the annual rainfall trends: a positive trend for
318 the summer dominated tropical monsoonal north, and a negative trend for the autumn/winter frontal

system dominated south. Tropical rainfall in northern Australia is summer (DJF) dominant and has been increasing over the last half a century. With little rain occurring in the winter (JJA) in these areas, the trend observed in winter is negligible, and the annual trend is dominated by changes in summer rainfall. In general summer rainfall has been increasing across Australia, but this trend is less clear in the east, for example isolated coastal areas on the east coast exhibit decreases in summer rainfall. The annual trend in rainfall for the south-west is strongly influenced by decreasing winter rainfall. In the south-east of Australia, a similar trend is observed – there is a decline in winter rainfall (though the largest observed decrease is for autumn rainfall) resulting in decreased mean annual rainfalls. Although trends are presented for all of Australia, we note that the rainfall gauging network in the arid center of Australia is limited, with high uncertainty in these areas. Hence the interpretation of results is limited to coastal, more populous, and streamflow producing regions.

Notionally, trends in PET could be expected to be proportional to changes in temperature or inversely proportional to rainfall due to increased cloud cover. But as discussed in the introduction there are many confounding factors and interdependencies affecting PET trends. Figure 5 presents, for the period 1960-2017, decreases in PET across the western half of Australia in summer and increases across the eastern half of Australia. There is a slight decrease in PET for the winter months in southern Australia and an increase in PET in northern Australia, but overall, the annual trend from east to west appears dominated by the trend in summer PET. There is little evidence for a spatial correlation of these trends with changes in rainfall or the increase in temperature observed across Australia over the past half a century. However, it should be noted that the driving radiation and wind variables for the PET simulated here are based on climatologies pre 1990 and 1975 respectively.


Annual
Summer (DJF)
Winter (JJA)
Rainfall
-PET
AET
SM
Runoff
−50 −20 −10 −5 −2 −1 0 1 2 5 10 20 50
Trend (mm/decade)

341

Figure 5. Linear trend in rainfall, potential evapotranspiration (PET), actual evapotranspiration (AET), soil moisture (SM), and runoff from 1960 to 2017. Results are presented annually, for the austral summer months (DJF), and the austral winter (JJA). Note that we plot -PET here for ease of visual colour comparison.

The modelled AET displays very similar trends to the rainfall, confirming that, with the exception of some coastal areas (primarily the south-east cost), evapotranspiration across most of Australia is water (and not energy) limited. In the summer months there is an increase in evapotranspiration across the tropical north, with decreases elsewhere. In the winter, there is a strong spatially coherent signal in the evapotranspiration, with decreases in the south-west, corresponding to decreases in availability of moisture due to declines in rainfall. The result is an annual trend in AET and rainfall of similar magnitude, between 10-50 mm/decade in the central northern tropics with decreases of a similar magnitude in the south-west of Australia.

For consistency, the units of the soil moisture trends are the same. As soil moisture trends are presented for the top 1m of soil, the magnitude of the trend may be less, despite its large modulating effect on flood response (Wasko and Nathan, 2019a). Soil moisture tends towards wetting in the summer in the north and west of Australia, with a drying trend only present in the south-west and south-east. In the winter there is almost universal drying across the south of Australia resulting in an annual trend similar to rainfall and AET trends. There are increases in soil moisture in the north of Australia and decreases in the south, consistent with trends in rainfall and water availability. However, arguably, the changes in soil moisture are more spatially consistent, an indicator of the longer residence time of water in the soil. For example, the drying trend across the east coast in soil moisture is much more extensive compared to the AET trend comprised of a mixture of increasing and decreasing trends.

The observed changes (trends) in rainfall and soil moisture translate to large changes in runoff across Australia. In the central tropics there is an increase in runoff in the summer of over 50mm/decade, while along the south-east coast there is a small drying trend of approximately 5-10mm/decade. In winter, the south-east and south-west coasts exhibit large decreasing trends in the order of 20mm/decade. In the north, winter is the dry season and there are no significant trends. The high spatial resolution of AWRA-L results in regional differences being modelled. For example, for Tasmania, the island off the south-east coast of Australia, a decreasing trend is modelled on the east-coast, and increasing trend on the west-coast, commensurate with the orographic divide that runs north-south. Similarly, across the south-east coast of Australia greater decreasing trends in runoff are observed on the coastal side of the dividing

mountain range that runs along the east coast. There is little trend in runoff elsewhere, with most trends in runoff across Australia contained to the coastal areas of higher rainfall.

3.3 Trends in high flow indices

The continental pattern across Australia for the 90th percentile (q90) of daily runoff (on an annual basis) and the 5-day maxima from 1960 to 2017 are presented in Figure 6. The trends in the 90th percentile runoff (top row) reflect the mean runoff trends presented in Figure 5, suggesting a uniform directional shift in the flow distribution, similar to global studies (Gudmundsson et al., 2019). There are decreases for q90 in the summer months (DJF) for the tropical north and parts of the south-east coast. Although rainfall and runoff are summer dominant along the north-east coast the trends are mixed and there is little trend elsewhere due to low summer rainfall. For winter months (JJA) there are large reductions in q90 across the southern coast of Australia with little trend elsewhere, coinciding with the lack of rainfall and runoff across the northern parts of Australia in the winter. On a continental scale, the annual trend reflects the summation of the seasonal patterns.

The 5-day annual maxima (bottom row) is more extreme than the 90th percentile and hence the trends exhibit greater variability than the trends for q90. Compared to the trend in q90 there are now more increases in the extreme runoff on the south-east coast reflecting how the more extreme the rainfall, the more likely we are to see increases, particular in the winter months when rainfall seasonality is dominant across south-west Australia. The annual trends form a different composite of the results presented for the 90th percentile. In the summer months the trend in the 5-day annual maxima remains similar to q90, but for winter the trends exhibit more variability with more wetting trends exhibited on the south-east coast of Australia. The 5-day maxima for eastern inland areas of Australia is influenced more by trends in the summer (and not winter) months while the northern part of Australia is influenced by the summer trends.

Despite predicted increases in extreme rainfall across Australia (Guerreiro et al., 2018) there remain large parts of the country with observed decreasing trends in q90 and the 5-day annual runoff maxima. This indicates that events at this level of severity are controlled by other processes than simply changes in extreme rainfall, for example changing rainfall persistence characteristics and changing soil moisture (e.g. Wasko and Nathan, 2019a). The mean runoff drying trend (Figure 5) is strongest in the south-west of Australia and this continues to be reflected with the q90 and 5-day annual maxima decreasing uniformly on the south-west coast (Figure 6).

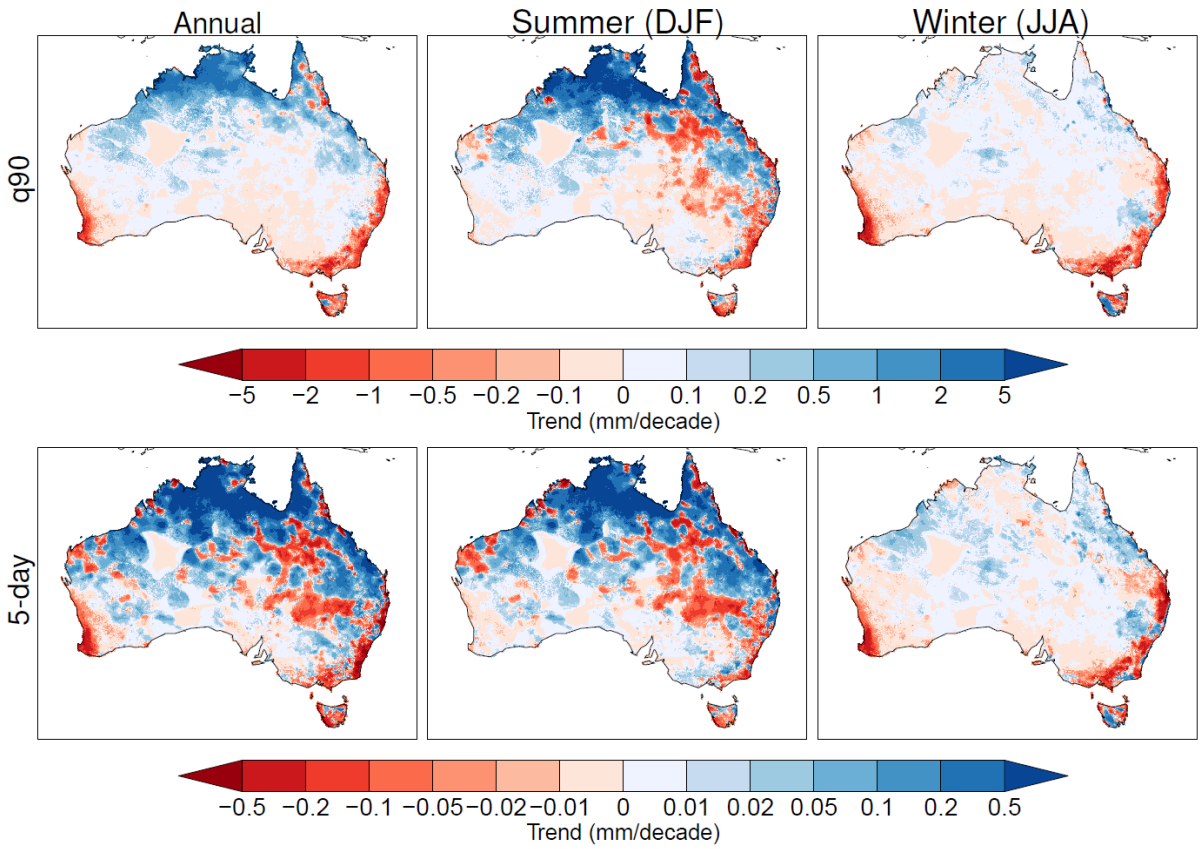


Figure 6. Linear trend in 90th percentile (q90) and annual maxima (5-day) for runoff from 1960 to 2017. Results are presented annually, for the austral summer months (DJF), and the austral winter (JJA).

3.4 Trends in low flow indices

Drought, or low flow, trends are quantified using the SRI-12 (Figure 7). SRI drought is relative to the variability at the individual pixel, hence by definition large parts of Australia will experience drought although they may not necessarily experience small mean rainfall. This is a limitation of using the SRI to characterise drought, particularly in regions of low flow (such as the arid interior of Australia). Correspondingly, we focus our analysis on the northern and coastal regions.

The SRI-12 is trending towards drier conditions around and inland of the southern half of the continent (Figure 7a) consistent with decreased runoff/streamflow (Figure 5). Across the Southern Slopes and Southern and South-Western Flatlands, there is a consistent negative trend in the SRI-12 indicating a shift to drier conditions and more frequent drought conditions. There is no single indicator of drought (Kiem et al., 2016), hence these results should be interpreted with respect to the trends in hydroclimatic

variables presented in Figure 5. What is starkly different from the previous results is that not just the south-west and south-east of Australia are trending towards drier conditions but most of southern Australia is experiencing drier conditions. This points to how multiple indicators of drying conditions, in the context of internal variability, need to be considered (e.g. Nathan et al., 2019).

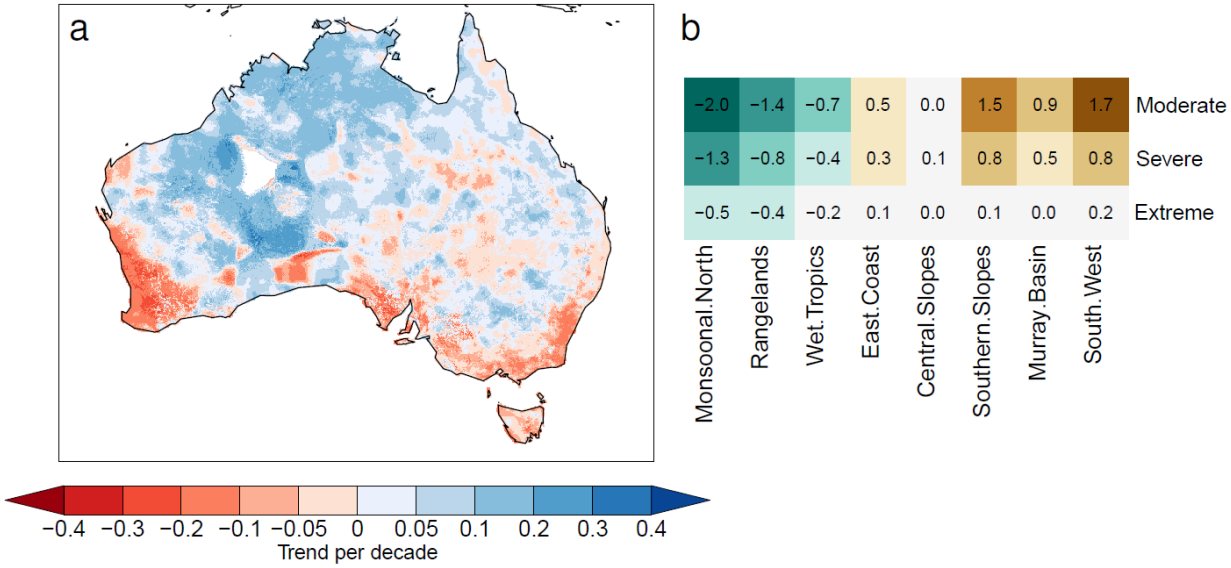


Figure 7. Trend in annual SRI from 1960 to 2017 (a) continental trends (b) change in the proportion (%/decade) of grid cells experiencing drought based on annual SRI (Table 1). Increases are shaded in brown and decreases are shaded in green.

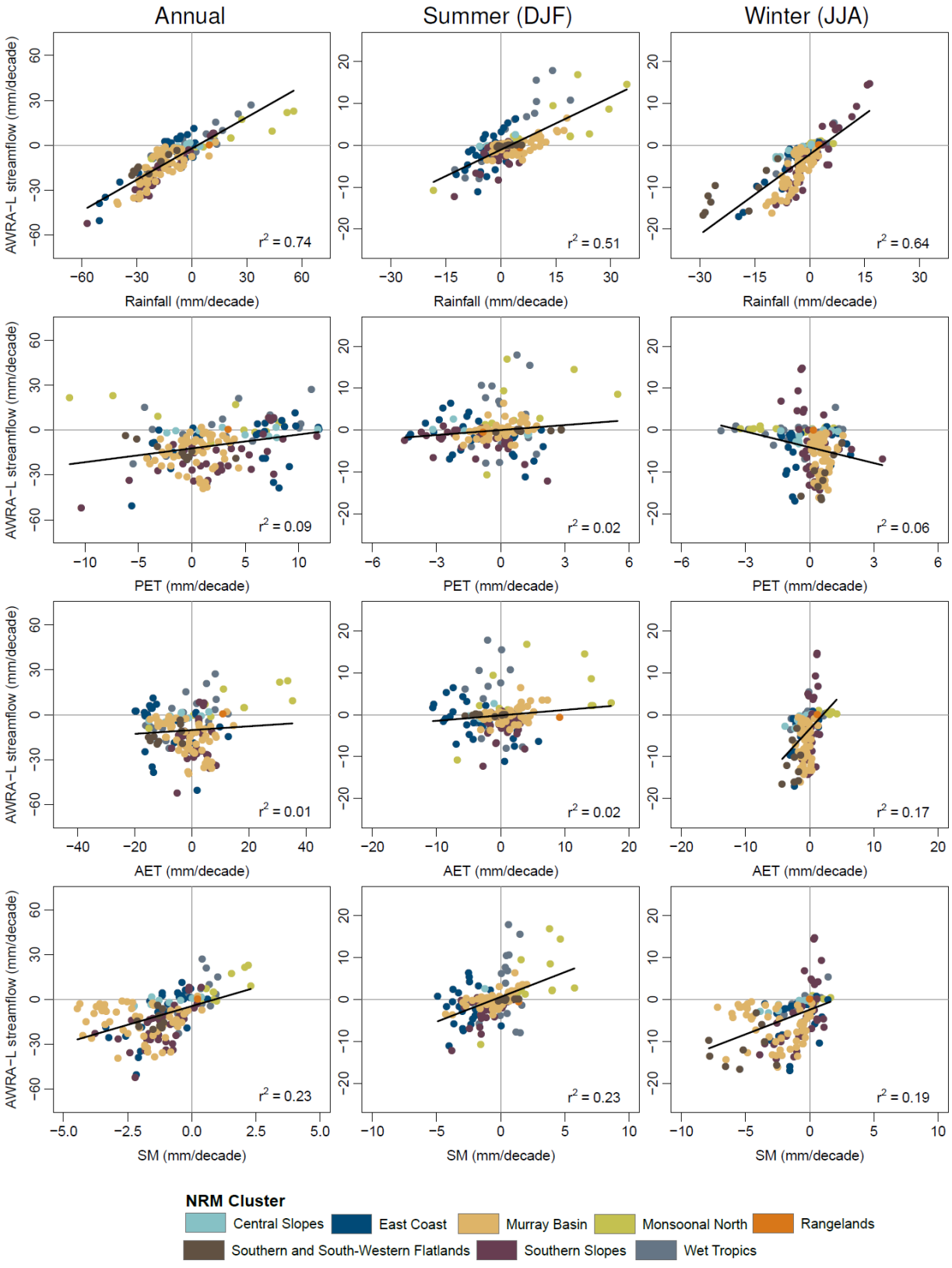
As an indicator of changes in drought extent, the change in the percentage of grid cells experiencing drought in each year in each of the NRM regions was calculated (Figure 7b). A 1% per decade increase represents an increase in the percentage of grid cells in an NRM observing drought (e.g. from 25% to 26%). The decreasing number of cells in the Monsoonal North, Rangelands, and Wet Tropics suggests a smaller extent of drought with climate change, consistent with the increases in mean rainfall presented in Figure 5. But we note that there were localised regions trending to lower SRI-12 (i.e. drought) in the Wet Tropics (Figure 7a). The greatest increase in the number of cells experiencing drought occurs in the Southern Slopes, Murray Basin and Southern and South-Western Flatlands. The large increasing extent of drought and decreasing mean annual rainfall in the Murray Basin is concerning, as this is a significant agricultural region for Australia.

3.5 Catchment scale interaction of hydroclimatological variables

Section 3.2 presented a continental scale analysis of changes in the drivers of streamflow across Australia. However, trends and interactions of hydroclimatological variables at the catchment scale are likely to differ from those at the continental scale (Saft et al., 2015; Whitfield, 2012). Focusing on streamflow, Figure 8 presents simulated streamflow trends against trends in observed rainfall and simulated PET, AET, and soil moisture. We note that simulated streamflow is a summation of the AWRA-L runoff (Section 2.2.2).

There is a strong correspondence between rainfall and simulated streamflow trends both seasonally and annually, with an r^2 of 0.74 at the annual timescale. It is very evident that the strongest positive trends in streamflow and rainfall occur in the Wet Tropics and Monsoonal North, and largely in the wet season (austral summer) months (DJF). Conversely the decrease in streamflow in the Southern and South-Western Flatlands is largely a result of winter (JJA) rainfall declines. This confirms the findings presented in the gridded results in Figure 5. But it is now also clear, which was not evident previously, that the Southern Slopes and Murray Basin regions, although adjacent, have markedly different behavior as a result of an orographic divide. Although mean annual rainfall and streamflow are reducing across both regions at the annual scale, summer rainfall and streamflow are increasing in the Murray Basin. In the winter the Southern Slopes have increasing rainfall and streamflow.

455


Annual
Summer (DJF)
Winter (JJA)
AWRA−L streamflow (mm/decade)
Rainfall (mm/decade)
PET (mm/decade)
AET (mm/decade)
SM (mm/decade)
r² = 0.74
r² = 0.51
r² = 0.64
r² = 0.09
r² = 0.02
r² = 0.06
r² = 0.01
r² = 0.02
r² = 0.17
r² = 0.23
r² = 0.23
r² = 0.19
NRM Cluster
Central Slopes
East Coast
Murray Basin
Monsoonal North
Rangelands
Southern and South-Western Flatlands
Southern Slopes
Wet Tropics

456

Figure 8. Simulated streamflow trend per decade for 160 catchments across Australia from 1960 to 2017 against trend in potential evapotranspiration (PET), actual evapotranspiration (AET), and soil moisture (SM). Results are presented annually, for the austral summer months (DJF), and the austral winter (JJA). Catchment locations are shown in Figure 2. A line of best fit is presented in black with the coefficient of determination (r^2) for each pair of variables. Coefficients of determination for individual NRM regions are presented in Table S1.

Similar to the continental trends, there is little correspondence between PET and runoff at catchment scale. This is because, firstly, the trend in PET is only realised as a trend in either AET, soil moisture, or runoff if there is sufficient moisture available (and it will appear in AET and soil moisture before runoff which is an integration of the above fluxes). Secondly, the trends in PET are small compared to rainfall. Despite strong continental coherence in AET and runoff trends (Figure 5), regional scale trends between AET and runoff generally have very low coefficients of determination (Table S1) with the exception of the Wet Tropics, Monsoonal North and Southern and South-Western Flatlands. This suggest, for these regions, greater runoff is correlated with greater evapotranspiration probably due to greater water availability through greater precipitation. The Wet Tropics, Monsoonal North, and Southern and South-Western Flatlands are wetter coastal regions and therefore are possibly not moisture limited but energy limited. However, regions like the Southern Slopes and East Coast are also coastal, and do not have a strong relationship between AET and runoff (annually), implying, not all coastal regions are energy limited. It does not appear that AET is driving changes in streamflow, as the strong positive relationship between AET and runoff for the Southern and South-Western Flatlands is counter to the fact that runoff is decreasing in this region reducing water availability.

Soil moisture is more strongly linked to streamflow (r^2 of 0.23 annually) than AET (r^2 of 0.01) or PET (r^2 of 0.09), suggesting wet soils are contributing to runoff and vice versa. The strength of these relationships does not necessarily correspond to the seasonality of streamflow. For example, there is a strong relationship in the summer months in the Murray Basin between runoff and soil moisture (r^2 of 0.40) and similarly for the Southern and South-Western Flatlands (r^2 of 0.49) but these are the months of the lowest streamflow. For winter streamflow, the relationship between soil moisture and streamflow is more random, suggesting that streamflow depends more on rainfall in wetter months whereas in drier months the relationship between streamflow and rainfall is modulated by soil moisture.

The lack of relationships in trend between soil moisture and runoff in the winter months for the Murray Basin and Southern and South-Western Flatlands is reflected in the annual relationship where little

correspondence exists between soil moisture and runoff trends with r^2 values less than 0.1 (Table S1). The East Coast and Central Slopes show strong positive annual associations between streamflow and soil moisture of 0.34 and 0.57 respectively suggesting the east coast of Australia has a strong relationship with soil moisture and runoff which was not present for the other variables. Although we can conclude that rainfall changes are the dominant driver of changes in streamflow, soil moisture is a secondary driver with the strength of the interaction between soil moisture and runoff varying strongly with season.

3.6 Catchment scale interaction of hydroclimatological variables for high flows

Figure 9 presents trends in the 90th percentile of annual catchment streamflow (q90) against the trends in the 90th percentile of rainfall (p90), trends in soil moisture, and trends in mean rainfall from 1960 to 2017. Due to the small correlations of runoff trend to trends in PET and AET, and the shorter time scale of high flows, the trends in PET and AET are omitted here. At an annual aggregation, the association between q90 and p90 trends (0.38) is poorer than that of q90 with the mean rainfall (0.68). For each NRM region the coefficient of determination is greater than 0.5 between q90 and mean rainfall (Table S2). There exists variability between regions for the relationship between trends in q90 and p90 but in general the strongest relationships exist between q90 and the mean rainfall (compared to p90 or soil moisture).

Seasonally, a strong relationship exists between trends in q90 and p90 across most regions. The relationship between the trends in q90 and p90 appears weaker than the correlation between the trends for mean rainfall and mean streamflow presented in Figure 8. This could be expected due to greater variability in the more extreme flows and rainfalls, compared to mean flows and rainfalls. There is a weak relationship between q90 and p90 trends in summer (DJF) for the Southern and South-Western Flatlands and Southern Slopes (< 0.1), possibly due to the fact that this is not the dominant streamflow season, and streamflow is baseflow dominated, resulting in higher associations with soil moisture (Table S2) up to 0.65 for the Southern and South-Western Flatlands .

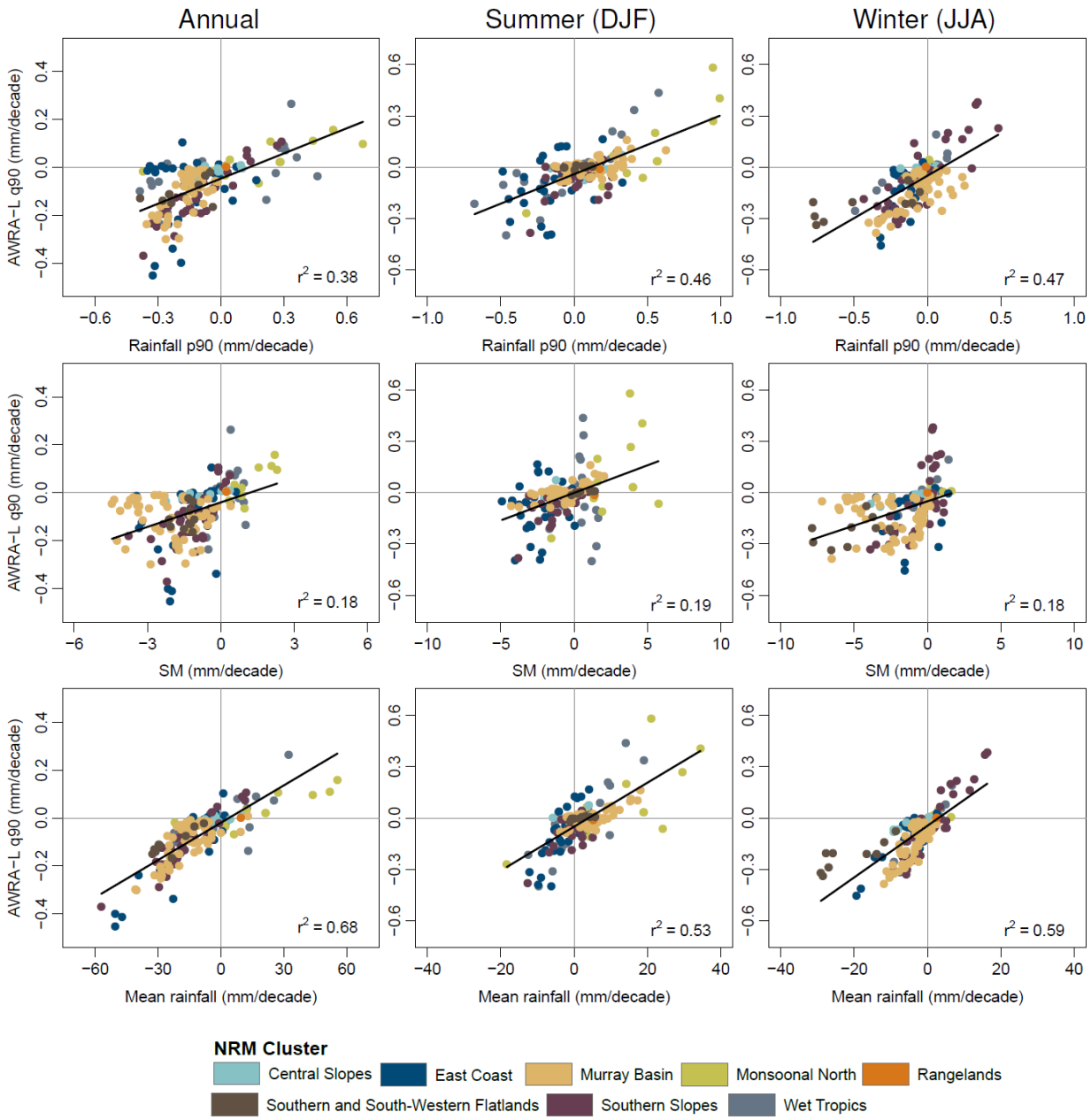


Figure 9. Modelled q90 streamflow runoff trend per decade for 160 catchments across Australia against p90 rainfall, soil moisture (SM), and mean rainfall. Results are presented annually, for the austral summer months (DJF), and the austral winter (JJA). Catchment locations are shown in Figure 2. The black line is a line of best fit with the coefficient of determination (r2) for each panel. Table S2 presents coefficients of determination for individual NRM regions.

There are quite large positive and negative trends in the Wet Tropics: q90 runoff with a strong association to p90, up to 0.73 in the Wet Tropics for the summer season. In the Monsoonal North q90 is generally increasing with increasing p90 (r^2 of 0.78). This is consistent with significant infiltration excess dominated high flows during the monsoonal wet (DJF) season. For winter (JJA), the strongest positive trends in q90 are observed in the Southern Slopes, and the strongest negative trends in the Southern and South-Western Flatlands, with an r^2 with the p90 trends of 0.67 and 0.55 respectively. The contrast to the summer trends in this region being dominated by soil moisture changes demonstrates how changing high (q90) runoff, as compared to mean runoff, is more linked to seasonality changes, and changes in seasonal extremes may not necessarily translate to change in the annual mean. For example, for the Murray Basin and Southern and South-Western Flatlands the summer association with soil moisture is greater than that with p90. Comparing an r^2 of 0.65 for the South and South-Western Flatlands between q90 and soil moisture with an r^2 of 0.09 for q90 and p90 demonstrates two points: first, high flows in seasons of low rainfall are more related to soil moisture changes than extreme rainfall changes; second, seasonal changes in high flows, out of sync with the maximum seasonality of flow, are dominant in this region. To summarise, for the Murray Basin and Southern and South-Western Flatlands, soil moisture and the mean climate state have a greater impact on changing high flows than changes in extreme rainfall.

Overall, the greatest association for trends in q90 is with trends in mean annual rainfall (Table S2). This doesn't necessarily imply that mean rainfall changes are driving high flow changes, but, as extreme rainfall changes constitute a large part of the volume of mean rainfall, we know that mean rainfall changes are highly dependent on changes in extreme rainfall. Moreover, mean rainfall changes are a larger driver of changes in soil moisture. Hence the trends in p90 rainfall and soil moisture are integrated into changes in the mean rainfall and the association between q90 and mean rainfall trends (Figure 9) is similar to the association between mean runoff and mean rainfall (Figure 8). Trends in q90 are similar to trends in mean runoff confirming that the direction (positive or negative) of trend in the entire runoff distribution is the same.

4 Discussions and Conclusions

We presented the first high-resolution evaluation of trends in key hydroclimatic variables across the terrestrial water balance for the Australian continent. Compared to the gauging network of (daily) rainfall observations, other hydrological variables such as evaporation, soil moisture, and streamflow (not affected by human interaction/management) are much more sparsely measured, meaning most studies of hydroclimatic trends are limited to rainfall and infer impacts to other parts of the water cycle from the

rainfall trends (e.g. Gallant et al., 2007). However, inferring trends in streamflow from rainfall alone can be problematic due to the complex interactions present at catchment scale (e.g. Sharma et al., 2018). Because of this, to quantify and understand changes in the hydrologic cycle both on the continental scale, and in ungauged catchments, modelling is required. Here, we used the Australian Water Resource Assessment model (AWRA-L) to study trends in rainfall, evapotranspiration, soil moisture, and runoff, as well as indicators of flooding and drought across the continent.

4.1 Evaluation of AWRA-L

AWRA-L has been extensively evaluated for its performance in simulating soil moisture and runoff, indicating its suitability for national water balance studies. We additionally evaluated the performance of AWRA-L to simulate trends in catchment aggregated runoff, that is, the streamflow. Simulated annual flow direction matched observations at 76% of the catchments with a coefficient of determination 0.38, indicating good performance across the continent. Localised decreases in observed streamflow along the north-east coast and at the very far south-west tip of the continent may be due to the fact that there is one set of parameters applied nationally with local behaviour modulated according to input static grids of landscape characteristics. This approach inevitably leads to areas where performance and behaviour does not follow observed data (due to input uncertainties and errors along with poor local parameterisation). However, as the performance of AWRA-L in ungauged basins approaches that of locally calibrated models for streamflow, this gives confidence in the use of AWRA-L nationally (Frost and Wright, 2018)

Overall, good correspondence with observed trends was found in the south-east of Australia, in particular in the Murray Basin and Southern Slopes NRM regions where observed drying trends are the largest. Reasonable correspondence between modelled and observed trends in streamflow was found in the northern parts of Australia for the warmer months when streamflow is greatest but on an annual basis, the coefficient of determination was less than 0.1 in the tropics. The large variability in the magnitude of the modelled trend in the tropics may be in part due to drainage currently being overly dependent on saturated conductivity, and not enough on rainfall variability in the gridded rainfall driving the model. But it should also be noted that this region generally has catchments which are larger in area and ephemeral leading to greater variability in observed trends.

4.2 Trends in hydroclimatic variables across Australia

Linear trends show that, consistent with the tropics expanding poleward (Grise et al., 2018; Staten et al., 2018), there has been increasing precipitation in the tropics and decreasing precipitation in the sub-

tropics, with trends to wetter conditions in the monsoon-dominated summer months in the north and drier conditions in the south in the winter months. As changes in rainfall corresponds to the dominant rainfall seasonality for Australia, on a continental scale there is correspondence between the trends in rainfall, AET, soil moisture and runoff since 1960. There is little correspondence between PET and AET trends with the primary (only) exception some limited regions on the south-east coast. The divergence of PET and AET trends fits with the fact that Australia as a whole is a moisture limited environment (Anabalón and Sharma, 2017)**.**

Consistent with extreme rainfalls (by volume) contributing most to the mean rainfall distribution (Taschetto and England, 2009; Wasko and Nathan, 2019b) and the entire flow distribution trending in the same direction with climate change (Gudmundsson et al., 2019), trends in the 90th percentile of runoff are largely related to changes in mean rainfall. Decreases in high flows (an indicator of flooding) are the greatest in the south-west and south-east coastal regions of Australia. But more severe flow extremes, such as the 5day annual maxima flow, exhibit less negative trends, suggesting the more extreme the flow event, the more likely it is to be increasing (Wasko and Nathan, 2019a).

Indicators of drought suggest a shift to more frequent occurrences (and more widespread) drought across large parts of Australia. Although shifts to more frequent drought conditions are largely contained to the Southern Slopes, South and South-Western Flatlands, and Murray Basin, there is evidence that parts of the tropics will also experience increasing drought, despite increases in rainfall. Although the eastern half of the Southern and South-Western Flatlands did not exhibit strong trends in decreasing runoff, there was a large decrease in the SRI-12 indicating a shift to more drought conditions. This is consistent with increasing variability in rainfall (Rajah et al., 2014) rather than changes in total mean rainfall causing greater restrictions to seasonal water supply (Nguyen et al., 2020).

Despite strong visual correlation between trends in rainfall, soil moisture, evapotranspiration and runoff at the continental scale, annual streamflow trends at the regional scale show the greatest association to rainfall trends with an r^2 of 0.74. This suggests rainfall changes are driving changes in streamflow and soil moisture is a secondary driver (r^2 of 0.23 annually). In the dry summer months, the associations of runoff and soil moisture (r^2 of 0.40) for the Murray Basin are similar to that between runoff and rainfall (r^2 of 0.49). This presents that soil moisture changes are a secondary driver of streamflow trends, except in dry months, where soil moisture is equally a primary driver.

For the 90th percentile of streamflow, trends were more closely aligned to mean rainfall changes (r^2 of 0.68) rather than the 90th percentile of rainfall (r^2 of 0.38). As extreme rainfall changes constitute a large part of the volume of mean rainfall change, the 90th percentile of rainfall and soil moisture are integrated into changes in mean rainfall. This suggests that trends in high flows are modulated by both rainfall and soil moisture changes. Indeed for the dry summer months in the Murray Basin and Southern and South-Western Flatlands, the association with soil moisture is greater than that with p90, indicating how high flows in seasons of low rainfall are more related to changes in soil moisture than extreme rainfall changes, with the converse true for the high rainfall season.

4.3 Implications and future work

Here we successfully performed a trend analysis of key hydrologic variables from 1960 to 2017 using continental scale water balance model (AWRA-L). We found trends towards greater rainfalls and water availability in the tropics with declines in rainfall and water availability in the south of the continent. While there is evidence of increasing extreme rainfalls across Australia, annual maxima flooding has decreased across large parts of the county. Declining rainfalls and streamflow in southeast Australia have resulted in increasing droughts affecting agriculture and water supply and if these trends are to continue, we can expect consequences to be further exacerbated.

Future work will focus on better understanding the impacts of climate change on water supply across Australia and the impact of changes in seasonality on drought and flooding. Localised projections of the impacts of changing hydrologic conditions on water supply exist for Australia (Henley et al., 2019; Nguyen et al., 2020), but we envisage that projections of AWRA-L will enable the development of more extensive studies that lead to greater understanding and a more holistic picture of the impacts of climate change on flooding and water supply across Australia.

Acknowledgements

Conrad Wasko receives funding from the University of Melbourne McKenzie Postdoctoral Fellowship scheme and Australian Research Council (ARC) Discovery Project DP200101326.

References

Albergel, C., Dorigo, W., Reichle, R.H., Balsamo, G., de Rosnay, P., Muñoz-Sabater, J., Isaksen, L., de Jeu, R., Wagner, W., 2013. Skill and Global Trend Analysis of Soil Moisture from Reanalyses and Microwave Remote Sensing. J. Hydrometeorol. 14, 1259–1277. https://doi.org/10.1175/JHM-D-12-

0161.1

Alexander, L.V., Hope, P., Collins, D., Trewin, B., Lynch, A., Nicholls, N., 2007. Trends in Australia's climate means and extremes: a global context. Aust. Meteorol. Mag. 56, 1–18. https://doi.org/10.1029/2005JD006119Alexander

Alexander, L. V., Arblaster, J.M., 2017. Historical and projected trends in temperature and precipitation extremes in Australia in observations and CMIP5. Weather Clim. Extrem. 15, 34–56. https://doi.org/10.1016/j.wace.2017.02.001

Allan, R.P., Barlow, M., Byrne, M.P., Cherchi, A., Douville, H., Fowler, H.J., Gan, T.Y., Pendergrass, A.G., Rosenfeld, D., Swann, A.L.S., Wilcox, L.J., 2020. Advances in understanding large-scale responses of the water cycle to climate change. Ann. N. Y. Acad. Sci. 1–27. https://doi.org/10.1111/nyas.14337

Allen, M.R., Ingram, W.J., 2002. Constraints on future changes in climate and the hydrologic cycle. Nature 419, 224–232. https://doi.org/10.1038/nature01092

Anabalón, A., Sharma, A., 2017. On the divergence of potential and actual evapotranspiration trends: An assessment across alternate global datasets. Earth's Futur. 5, 905–917. https://doi.org/10.1002/2016EF000499

Andersson, J.C.M., Pechlivanidis, I.G., Gustafsson, D., Donnelly, C., Arheimer, B., 2015. Key factors for improving large-scale hydrological model performance. Eur. Water 49, 77–88.

Asadi Zarch, M.A., Sivakumar, B., Sharma, A., 2015. Droughts in a warming climate: A global assessment of Standardized precipitation index (SPI) and Reconnaissance drought index (RDI). J. Hydrol. 526, 183–195. https://doi.org/10.1016/j.jhydrol.2014.09.071

Ball, J., Babister, M., Nathan, R., Weeks, W., Wienmann, R., Retallick, M., Testoni, I. (Eds.), 2019. Australian Rainfall and Runoff: A Guide to Flood Estimation. Commonwealth of Australia.

Beck, H.E., Wood, E.F., Pan, M., Fisher, C.K., Miralles, D.G., van Dijk, A.I.J.M., McVicar, T.R., Adler, R.F., 2019. MSWEP V2 Global 3-Hourly 0.1° Precipitation: Methodology and Quantitative Assessment. Bull. Am. Meteorol. Soc. 100, 473–500. https://doi.org/10.1175/BAMS-D-17-0138.1

Becker, A., Finger, P., Meyer-Christoffer, A., Rudolf, B., Schamm, K., Schneider, U., Ziese, M., 2013. A description of the global land-surface precipitation data products of the Global Precipitation Climatology Centre with sample applications including centennial (trend) analysis from 1901-

present. Earth Syst. Sci. Data 5, 71–99. https://doi.org/10.5194/essd-5-71-2013

Berghuijs, W.R., Harrigan, S., Molnar, P., Slater, L.J., Kirchner, J.W., 2019. The Relative Importance of Different Flood-Generating Mechanisms Across Europe. Water Resour. Res. 2019WR024841. https://doi.org/10.1029/2019WR024841

Chiew, F.H.S., McMahon, T.A., 2002. Global ENSO-streamflow teleconnection, streamflow forecasting and interannual variability. Hydrol. Sci. J. 47, 505–522. https://doi.org/10.1080/02626660209492950

CSIRO & BOM, 2018. State of the Climate.

CSIRO, Bureau of Meteorology, 2015. Climate Change in Australia Projections for Australia's Natural Resource Management Regions: Technical Report.

Dey, R., Gallant, A.J.E., Lewis, S.C., 2020. Evidence of a continent-wide shift of episodic rainfall in Australia. Weather Clim. Extrem. 29, 100274. https://doi.org/10.1016/j.wace.2020.100274

Dey, R., Lewis, S.C., Arblaster, J.M., Abram, N.J., 2019. A review of past and projected changes in Australia's rainfall. Wiley Interdiscip. Rev. Clim. Chang. 10, 1–23. https://doi.org/10.1002/wcc.577

Do, H.X., Westra, S., Leonard, M., 2017. A global-scale investigation of trends in annual maximum streamflow. J. Hydrol. 552, 28–43. https://doi.org/10.1016/j.jhydrol.2017.06.015

Donat, M.G., Alexander, L. V., Yang, H., Durre, I., Vose, R., Dunn, R.J.H., Willett, K.M., Aguilar, E., Brunet, M., Caesar, J., Hewitson, B., Jack, C., Klein Tank, a. M.G., Kruger, a. C., Marengo, J., Peterson, T.C., Renom, M., Oria Rojas, C., Rusticucci, M., Salinger, J., Elrayah, a. S., Sekele, S.S., Srivastava, a. K., Trewin, B., Villarroel, C., Vincent, L. a., Zhai, P., Zhang, X., Kitching, S., 2013. Updated analyses of temperature and precipitation extreme indices since the beginning of the twentieth century: The HadEX2 dataset. J. Geophys. Res. Atmos. 118, 2098–2118. https://doi.org/10.1002/jgrd.50150

Donohue, R.J., McVicar, T.R., Roderick, M.L., 2010. Assessing the ability of potential evaporation formulations to capture the dynamics in evaporative demand within a changing climate. J. Hydrol. 386, 186–197.

Elmahdi, A., Hafeez, M., Smith, A., Frost, A., 2016. Using an integrated continental hydrological model (AWRA modelling system) to inform australian water resources assessment, in: 37th Hydrology and Water Resources Symposium 2016: Water, Infrastructure and the Environment, HWRS 2016.

694 Fawcett, R., Trewin, B.C., Braganza, K., Smalley, R.J., Jovanovic, B., Jones, D.A., 2012. On the sensitivity of
695 Australian temperature trends and variability to analysis methods and observation networks,
696 CAWCR Technical Report No. 050.

697 Feng, H., Zhang, M., 2015. Global land moisture trends: Drier in dry and wetter in wet over land. Sci.
698 Rep. 5, 1–6. https://doi.org/10.1038/srep18018

699 Fowler, K.J.A., Peel, M.C., Western, A.W., Zhang, L., Peterson, T.J., 2016. Simulating runoff under
700 changing climatic conditions: Revisiting an apparent deficiency of conceptual rainfall-runoff
701 models. Water Resour. Res. 52, 1820–1846. https://doi.org/10.1002/2015WR018068

702 Frost, A.J.., Ramchurn, A.., Smith, A.., 2018. The Australian landscape water balance model (AWRA-L v6).
703 Technical Description of the Australian Water Resources Assessment Landscape model version 6.
704 Melbourne, Australia.

705 Frost, A.J., Wright, D.P., 2018. Evaluation of the Australian Landscape Water Balance model (AWRA-L
706 v6): Comparison of AWRA-L v6 against Observed Hydrological Data and Peer Models.

707 Frost, Andrew J., Wright, D.P., 2018. Evaluation of the Australian Landscape Water Balance model :
708 AWRA-L v6. A comparison of AWRA-L v6 against Observed Hydrological Data and Peer Models.
709 Melbourne, Australia.

710 Gallant, A.J.E., Hennessy, K.J., Risbey, J., 2007. Trends in rainfall indices for six Australian regions: 1910-
711 2005. Aust. Meteorol. Mag. 56, 223–239.

712 Grant, I., Jones, D., Wang, W., Fawcett, R., Barratt, D., 2008. Meteorological and remotely sensed
713 datasets for hydrological modelling: a contribution to the Australian Water Availability Project, in:
714 Catchment-Scale Hydrological Modelling and Data Assimilation (CAHMDA-3) International
715 Workshop on Hydrological Prediction: Modelling, Observation and Data Assimilation. Melbourne,
716 Australia.

717 Grise, K.M., Davis, S.M., Staten, P.W., Adam, O., 2018. Regional and seasonal characteristics of the
718 recent expansion of the tropics. J. Clim. 31, 6839–6856. https://doi.org/10.1175/JCLI-D-18-0060.1

719 Groisman, P.Y., Knight, R.W., Easterling, D.R., Karl, T.R., Hegerl, G.C., Razuvaev, V.N., 2005. Trends in
720 Intense Precipitation in the Climate Record. J. Clim. 18, 1326–1350.
721 https://doi.org/10.1175/JCLI3339.1

Gudmundsson, L., Leonard, M., Do, H.X., Westra, S., Seneviratne, S.I., 2019. Observed Trends in Global Indicators of Mean and Extreme Streamflow. Geophys. Res. Lett. 46, 756–766. https://doi.org/10.1029/2018GL079725

Guerreiro, S.B., Fowler, H.J., Barbero, R., Westra, S., Lenderink, G., Blenkinsop, S., Lewis, E., Li, X.-F., 2018. Detection of continental-scale intensification of hourly rainfall extremes. Nat. Clim. Chang. 8, 803–807. https://doi.org/10.1038/s41558-018-0245-3

Hafeez, M., Smith, A., Frost, A., Srikanthan, R., Barua, S., Elmahdi, A., 2015. The Bureau's Operational Australian Water Resources Assessment Modelling System (AWRAMS): From Science to End Users Applications and Future Directions, in: Modsim 2015 21st International Congress on Modelling and Simulation.

Hartmann, D.L., Klein Tank, A.M.G., Rusticucci, M., Alexander, L. V., Broennimann, S., Charabi, Y., Dentener, F.J., Dlugokencky, E.J., Easterling, D.R., Kaplan, A., Soden, B.J., Thorne, P.W., Wild, M., Zhai, P.M., 2013. Observations: Atmosphere and Surface, in: Stocker, T., Qin, D., Plattner, G.-K., Tignor, M., Allen, S.K., Boschung, J., Nauels, A., Xia, Y., Bex, V., Midgley, P.M. (Eds.), Climate Change 2013: The Physical Science Basis. Contribution of Working Group I to the Fifth Assessment Report of the Intergovernmental Panel on Climate Change. Cambridge University Press, Cambridge, UK and New York, NY, USA, pp. 159–254.

Henley, B.J., Peel, M.C., Nathan, R., King, A.D., Ukkola, A.M., Karoly, D.J., Tan, K.S., 2019. Amplification of risks to water supply at 1.5 °C and 2 °C in drying climates: a case study for Melbourne, Australia. Environ. Res. Lett. 14, 084028. https://doi.org/10.1088/1748-9326/ab26ef

Hill, P., Thomson, R., 2019. Chapter 3. Losses, Book 5: Flood Hydrograph Estimation:, in: Ball, J., Babister, M., Nathan, R., Weinmann, E., Retallick, M., Testoni, I. (Eds.), Australian Rainfall and Runoff - A Guide to Flood Estimation. Commonwealth of Australia.

Hill, P., Zhang, J., Nathan, R., 2016. Australian rainfall and runoff Revision Project 6: Loss models for catchment simulation. Barton, ACT.

Holgate, C.., De Jeu, R.A.M., van Dijk, A.I.J.., Liu, Y.., Renzullo, L.J., Vinodkumar, Dharssi, I., Parinussa, R.M., Van Der Schalie, R., Gevaert, A., Walker, J., McJannet, D., Cleverly, J., Haverd, V., Trudinger, C.M., Briggs, P.R., 2016. Comparison of remotely sensed and modelled soil moisture data sets across Australia. Remote Sens. Environ. 186, 479–500. https://doi.org/10.1016/j.rse.2016.09.015

751 Huntington, T.G., 2006. Evidence for intensification of the global water cycle: Review and synthesis. J.
752 Hydrol. 319, 83–95. https://doi.org/10.1016/j.jhydrol.2005.07.003

753 Ishak, E.H., Rahman, A., Westra, S., Sharma, A., Kuczera, G., 2013. Evaluating the non-stationarity of
754 Australian annual maximum flood. J. Hydrol. 494, 134–145.
755 https://doi.org/10.1016/j.jhydrol.2013.04.021

756 Ivancic, T.J., Shaw, S.B., 2015. Examining why trends in very heavy precipitation should not be mistaken
757 for trends in very high river discharge. Clim. Change 133, 681–693.
758 https://doi.org/10.1007/s10584-015-1476-1

759 Johnson, F., Sharma, A., 2010. A Comparison of Australian Open Water Body Evaporation Trends for
760 Current and Future Climates Estimated from Class A Evaporation Pans and General Circulation
761 Models. J. Hydrometeorol. 11, 105–121. https://doi.org/10.1175/2009JHM1158.1

762 Johnson, F., White, C.J., van Dijk, A., Ekstrom, M., Evans, J.P., Jakob, D., Kiem, A.S., Leonard, M.,
763 Rouillard, A., Westra, S., 2016. Natural hazards in Australia: floods. Clim. Change 139, 21–35.
764 https://doi.org/10.1007/s10584-016-1689-y

765 Jones, D., Wang, W., Fawcett, R., 2009. High-quality spatial climate data-sets for Australia. Aust.
766 Meteorol. Oceanogr. J. 58, 233–248.

767 Jung, M., Reichstein, M., Ciais, P., Seneviratne, S.I., Sheffield, J., Goulden, M.L., Bonan, G., Cescatti, A.,
768 Chen, J., de Jeu, R., Dolman, A.J., Eugster, W., Gerten, D., Gianelle, D., Gobron, N., Heinke, J.,
769 Kimball, J., Law, B.E., Montagnani, L., Mu, Q., Mueller, B., Oleson, K., Papale, D., Richardson, A.D.,
770 Roupsard, O., Running, S., Tomelleri, E., Viovy, N., Weber, U., Williams, C., Wood, E., Zaehle, S.,
771 Zhang, K., 2010. Recent decline in the global land evapotranspiration trend due to limited moisture
772 supply. Nature 467, 951–954. https://doi.org/10.1038/nature09396

773 Kharin, V. V., Zwiers, F.W., Zhang, X., Wehner, M., 2013. Changes in temperature and precipitation
774 extremes in the CMIP5 ensemble. Clim. Change 119, 345–357. https://doi.org/10.1007/s10584-
775 013-0705-8

776 Kiem, A.S., Johnson, F., Westra, S., van Dijk, A., Evans, J.P., O???Donnell, A., Rouillard, A., Barr, C., Tyler,
777 J., Thyer, M., Jakob, D., Woldemeskel, F., Sivakumar, B., Mehrotra, R., 2016. Natural hazards in
778 Australia: droughts. Clim. Change 139, 37–54. https://doi.org/10.1007/s10584-016-1798-7

King, A.D., Pitman, A.J., Henley, B.J., Ukkola, A.M., Brown, J.R., 2020. The role of climate variability in Australian drought. Nat. Clim. Chang. 10, 177–179. https://doi.org/10.1038/s41558-020-0718-z

Kirono, D.G.C., Hennessy, K.J., Grose, M.R., 2017. Increasing risk of months with low rainfall and high temperature in southeast Australia for the past 150 years. Clim. Risk Manag. 16, 10–21. https://doi.org/10.1016/j.crm.2017.04.001

Koutsoyiannis, D., 2020. Revisiting the global hydrological cycle: is it intensifying? Hydrol. Earth Syst. Sci. 24, 3899–3932. https://doi.org/10.5194/hess-24-3899-2020

Liu, Y., Liu, Y., Wang, W., 2019. Inter-comparison of satellite-retrieved and Global Land Data Assimilation System-simulated soil moisture datasets for global drought analysis. Remote Sens. Environ. 220, 1–18. https://doi.org/10.1016/j.rse.2018.10.026

Martinez-Villalobos, C., Neelin, J.D., 2018. Shifts in Precipitation Accumulation Extremes During the Warm Season Over the United States. Geophys. Res. Lett. 45, 8586–8595. https://doi.org/10.1029/2018GL078465

McKee, T.B., Doesken, N.J., Kleist, J., 1993. The relationship of drought frequency and duration to time scales, in: Eighth Conference on Applied Climatology. Anaheim, California. https://doi.org/10.1002/jso.23002

McMahon, T.A., Vogel, R.M., Peel, M.C., Pegram, G.G.S., 2007. Global streamflows - Part 1: Characteristics of annual streamflows. J. Hydrol. 347, 243–259. https://doi.org/10.1016/j.jhydrol.2007.09.002

McVicar, T.R., Van Niel, T.G., Li, L.T., Roderick, M.L., Rayner, D.P., Ricciardulli, L., Donohue, R.J., 2008. Wind speed climatology and trends for Australia, 1975-2006: Capturing the stilling phenomenon and comparison with near-surface reanalysis output. Geophys. Res. Lett. 35, 1–6. https://doi.org/10.1029/2008GL035627

Nathan, R.J., McMahon, T.A., Peel, M.C., Horne, A., 2019. Assessing the degree of hydrologic stress due to climate change. Clim. Change 156, 87–104. https://doi.org/10.1007/s10584-019-02497-4

Nguyen, H., Mehrotra, R., Sharma, A., 2020. Assessment of climate change impacts on reservoir storage reliability, resilience and vulnerability using a Multivariate Frequency Bias Correction approach. Water Resour. Res. 0–3. https://doi.org/10.1029/2019wr026022

807 Nguyen, H., Wheeler, M.C., Otkin, J.A., Cowan, T., Frost, A., Stone, R., 2019. Using the evaporative stress
808 index to monitor flash drought in Australia. Environ. Res. Lett. 14. https://doi.org/10.1088/1748-
809 9326/ab2103

810 Peel, M.C., McMahon, T.A., Finlayson, B.L., 2004. Continental differences in the variability of annual
811 runoff-update and reassessment. J. Hydrol. 295, 185–197.
812 https://doi.org/10.1016/j.jhydrol.2004.03.004

813 Penman, H.L., 1948. Natural Evporation from Open Water, Bare Soil and Grass. R. Soc. 193, 120–145.
814 https://doi.org/10.1098/rspa.1948.0037

815 Peterson, T.J., Wasko, C., Saft, M., Peel, M.C., 2020. AWAPer: An R package for area weighted catchment
816 daily meteorological data anywhere within Australia. Hydrol. Process. 34, 1301–1306.
817 https://doi.org/10.1002/hyp.13637

818 Potter, N.J., Chiew, F.H.S., Frost, A.J., 2010. An assessment of the severity of recent reductions in rainfall
819 and runoff in the Murray-Darling Basin. J. Hydrol. 381, 52–64.
820 https://doi.org/10.1016/j.jhydrol.2009.11.025

821 Rajah, K., O'Leary, T., Turner, A., Petrakis, G., Leonard, M., Westra, S., 2014. Changes to the temporal
822 distribution of daily precipitation. Geophys. Res. Lett. 41, 8887–8894.
823 https://doi.org/10.1002/2014GL062156

824 Risbey, J.S., Pook, M.J., McIntosh, P.C., 2013. Spatial trends in synoptic rainfall in southern Australia.
825 Geophys. Res. Lett. 40, 3781–3785. https://doi.org/10.1002/grl.50739

826 Saft, M., Peel, M.C., Western, A.W., Zhang, L., 2016. Predicting shifts in rainfall-runoff partitioning during
827 multiyear drought: Roles of dry period and catchment characteristics. Water Resour. Res. 52,
828 9290–9305. https://doi.org/10.1002/2016WR019525

829 Saft, M., Western, A.W., Zhang, L., Peel, M.C., Potter, N.J., 2015. The influence of multiyear drought on
830 the annual rainfall-runoff relationship: An Australian perspective. Water Resour. Res. 51, 2444–
831 2463. https://doi.org/10.1002/2014WR015348

832 Sharma, A., Wasko, C., Lettenmaier, D.P., 2018. If Precipitation Extremes Are Increasing, Why Aren't
833 Floods? Water Resour. Res. 54, 8545–8551. https://doi.org/10.1029/2018WR023749

834 Shukla, S., Wood, A.W., 2008. Use of a standardized runoff index for characterizing hydrologic drought.

Geophys. Res. Lett. 35, 1–7. https://doi.org/10.1029/2007GL032487

Staten, P.W., Lu, J., Grise, K.M., Davis, S.M., Birner, T., 2018. Re-examining tropical expansion. Nat. Clim. Chang. 8, 768–775. https://doi.org/10.1038/s41558-018-0246-2

Stephens, C.M., McVicar, T.R., Johnson, F.M., Marshall, L.A., 2018. Revisiting Pan Evaporation Trends in Australia a Decade on. Geophys. Res. Lett. 45, 11,164-11,172. https://doi.org/10.1029/2018GL079332

Sun, Q., Zhang, X., Zwiers, F., Westra, S., Alexander, L. V., 2020. A global, continental and regional analysis of changes in extreme precipitation. J. Clim. 1–52. https://doi.org/10.1175/JCLI-D-19-0892.1

Taschetto, A.S., England, M.H., 2009. An analysis of late twentieth century trends in Australian rainfall. Int. J. Climatol. 29, 791–807. https://doi.org/10.1002/joc.1736

Tramblay, Y., Mimeau, L., Neppel, L., Vinet, F., Sauquet, E., 2019. Detection and attribution of flood trends in Mediterranean basins. Hydrol. Earth Syst. Sci. 23, 4419–4431. https://doi.org/10.5194/hess-23-4419-2019

Van Dijk, A., 2010. The Australian Water Resources Assessment System. Technical Report 3. Landscape Model (version 0.5) Technical Description. CSIRO: Water for a Healthy Country National Research Flagship.

Van Dijk, A.I.J.M., Beck, H.E., Crosbie, R.S., De Jeu, R.A.M., Liu, Y.Y., Podger, G.M., Timbal, B., Viney, N.R., 2013. The Millennium Drought in southeast Australia (2001-2009): Natural and human causes and implications for water resources, ecosystems, economy, and society. Water Resour. Res. 49, 1040–1057. https://doi.org/10.1002/wrcr.20123

Viney, N., Vaze, J., Crosbie, R., Wang, B., Dawes, W., Frost, A., 2015. AWRA-L v5.0: technical description of model algorithms and inputs. https://doi.org/https://doi.org/10.4225/08/58518bc790ff7

Wasko, C., Nathan, R., 2019a. Influence of changes in rainfall and soil moisture on trends in flooding. J. Hydrol. 575, 432–441. https://doi.org/10.1016/j.jhydrol.2019.05.054

Wasko, C., Nathan, R., 2019b. The local dependency of precipitation on historical changes in temperature. Clim. Change 156, 105–120. https://doi.org/10.1007/s10584-019-02523-5

Wasko, C., Nathan, R., Peel, M.C., 2020. Changes in Antecedent Soil Moisture Modulate Flood

Seasonality in a Changing Climate. Water Resour. Res. 56, e2019WR026300. https://doi.org/10.1029/2019WR026300

Wasko, C., Sharma, A., Lettenmaier, D.P., 2019. Increases in temperature do not translate to increased flooding. Nat. Commun. 10, 5676. https://doi.org/10.1038/s41467-019-13612-5

Weedon, G.P., Balsamo, G., Bellouin, N., Gomes, S., Best, M.J., Viterbo, P., 2014. Data methodology applied to ERA-Interim reanalysis data. Water Resour. Res. 50, 7505–7514. https://doi.org/10.1002/2014WR015638.Received

Westra, S., Alexander, L., Zwiers, F., 2013. Global increasing trends in annual maximum daily precipitation. J. Clim. 26, 3904–3918. https://doi.org/http://dx.doi.org/10.1175/JCLI-D-12-00502.1

Whitfield, P.H., 2012. Floods in future climates: A review. J. Flood Risk Manag. 5, 336–365. https://doi.org/10.1111/j.1753-318X.2012.01150.x

Zeng, Z., Peng, L., Piao, S., 2018. Response of terrestrial evapotranspiration to Earth's greening. Curr. Opin. Environ. Sustain. 33, 9–25. https://doi.org/10.1016/j.cosust.2018.03.001

Zhang, X.S., Amirthanathan, G.E., Bari, M.A., Laugesen, R.M., Shin, D., Kent, D.M., MacDonald, A.M., Turner, M.E., Tuteja, N.K., 2016. How streamflow has changed across Australia since the 1950s: evidence from the network of hydrologic reference stations. Hydrol. Earth Syst. Sci. 20, 3947–3965. https://doi.org/10.5194/hess-20-3947-2016

Zhang, Y.Q., Viney, N., Chen, Y., Li, H.Y., 2011. Collation of streamflow dataset for 719 unregulated Australian catchments. CSIRO: Water for a Healthy Country National Research Flagship.